LABORATORY STUDIES OF WATER DROPLET EVAPORATION KINETICS

Alfred M. Moyle*, Paul M. Smidansky and Dennis Lamb
Department of Meteorology, The Pennsylvania State University, University Park, PA 16802

1. INTRODUCTION

Quantifying the response of a population of cloud droplets to their changing environment is fundamental to our understanding of warm-cloud microphysics. The exchange of water mass between the condensed phase and the vapor depends on droplet size and ambient conditions, and it controls the evolution of droplet size spectra that contribute to the development of precipitation. In spite of the importance of this process, considerable disagreement remains between the results of prior experimental studies, and the details of its mechanism are only partially understood.

In this study, carefully designed experiments were combined with particle-scale model calculations to provide insight into the physics of water mass accommodation. We utilized an electrodynamic particle trap to examine the evaporation of individual high-purity water droplets. Droplets in the radius range from 15 to 50 microns were injected into the particle trap, where Mie-scattering techniques were used to provide high-precision measurements of their size as a function of time. The properties of the gaseous environment (T, total pressure, and dew point) were well-characterized. Least-squares fitting of a kinetic mass growth model was used to extract values of the mass accommodation coefficient from the experimental data. The high quality of the least-squares fits demonstrates that the kinetic model provides an excellent description of the evaporation process.

2. THEORY OF DROPLET EVAPORATION

The mass rate of change of a water droplet in a steady state vapor field is given by (Pruppacher and Klett 1997, p. 506)

* Corresponding author address: Alfred M. Moyle, 503 Walker Building, Penn State University, University Park, PA 16802, USA. email: amm14@psu.edu.

$$\frac{dm}{dt}=\frac{4\pi a D_v^* M}{R}\left(\frac{p_\infty}{T_\infty}-\frac{p_{sat}}{T_a}\right) \qquad (1)$$

where a is the droplet radius, T_∞ is the ambient temperature, T_a is the droplet temperature, R is the universal gas constant, m is the mass of the droplet, M is the molar mass of water, p_∞ is the ambient partial pressure of H_2O, p_{sat} is its equilibrium vapor pressure, and D_v^* is the effective gas-phase diffusion coefficient (including surface kinetic effects).

Assuming that the enthalpy of H_2O evaporation is in balance with the thermal energy conducted to the drop by the surrounding gas, the droplet temperature may be expressed in the form of (Pruppacher and Klett 1997, p. 509)

$$T_a=T_\infty+\frac{L_e}{4\pi a k_g^*}\cdot\frac{dm}{dt} \qquad (2)$$

where L_e is the specific enthalpy of H_2O evaporation and k_g^* is the effective thermal conductivity of the surrounding gas (including surface kinetic effects).

In Equations (1) and (2), D_v^* and k_g^* have the forms of (Pruppacher and Klett 1997, p. 506, p. 509)

$$D_V^*=\frac{D_V}{\dfrac{a}{a+\Delta}+\dfrac{4D_V}{a\alpha\bar{v}_w}} \qquad (3)$$

$$k_g^*=\frac{k_g}{\dfrac{a}{a+\Delta}+\dfrac{4k_g}{a\alpha_T n_g C_p\bar{v}}} \qquad (4)$$

where D_v, α, and $\bar{v}_w$ are, respectively, the diffusion coefficient, mass accommodation coefficient, and mean molecular speed of H_2O, Δ is a distance on the order of one mean free path from the droplet surface, k_g, n_g, C_p, and $\bar{v}$ are, respectively, the thermal conductivity, number density, heat capacity,

and mean molecular speed of the ambient gas, while α_T is the thermal accommodation coefficient.

A FORTRAN computer code was developed to solve the coupled system of Equations (1) and (2). Simulations of the time-dependent droplet radius calculated for the specific experimental conditions in this study were compared with laboratory measurements in a least-squares analysis in order to extract the best fit value of the mass accommodation coefficient, α.

3. EXPERIMENTAL METHODS

Charged droplets were derived from HPLC reagent grade water (J. T. Baker, 'Baker Analyzed'). In each experimental run, an individual droplet was trapped by the AC field of a cubic electrodynamic levitation cell (Lamb et al. 1996). Each droplet was exposed to a well-characterized horizontal laminar flow of N_2 containing a known concentration of water vapor.
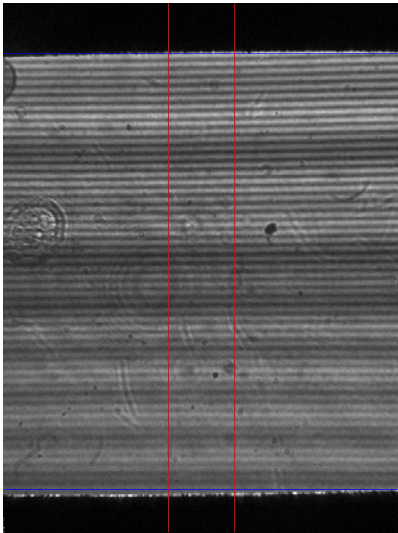

Figure 1. Video image of the Mie interference fringes from a pure water droplet between scattering angles of 80° and 100°. Horizontal blue lines mark the edges of the mask which determines the 20° field of view. Vertical red lines indicate the range of pixels averaged to obtain the fringe pattern in the upper panel of Figure 2.

The test particle was illuminated by an Ar^+ laser (Spectra Physics 165, 0.488

μm). Two optical systems were used to observe the droplet. The first consisted of a video camera and monitor which provided a focused image for position control. A second optical system was used to view and record Mie interference patterns (see Fig. 1).

Initial experiments used an analog system consisting of a video camera and VCR to record the fringe patterns for later analysis. Eventually, this system was replaced by a digital camera (Point Grey Research, Scorpion) which permitted streaming of video (640x480 pixel resolution at 60 frames per second) directly to a computer hard drive.
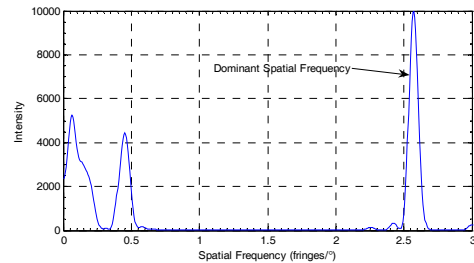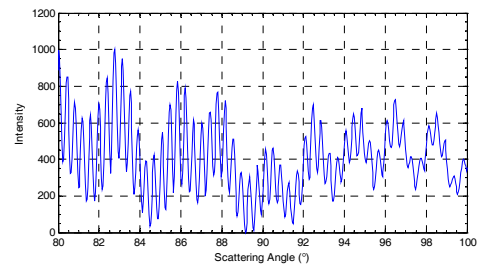

Figure 2. Upper panel: Fringe pattern for water droplet of Figure 1. Lower Panel: Fast Fourier Transform of the Mie interference fringes.

An individual video frame was used to determine the radius of the evaporating drop at one instant in time (Steiner et al. 1999). The intensity as a function of scattering angle (Fig. 2, upper panel) was Fourier-transformed in order to determine the dominant spatial frequency of the fringe pattern (Fig. 2, lower panel). A Mie computer code was used to generate a calibration of drop size versus dominant spatial frequency. The absolute size determined by this method was used as a reference for determining radii at other times by an integration method, which takes account of the property that the overall

intensity of the scattered light over the entire angle range attains a maximum for every 0.063 μm change in droplet radius for our optical setup (Xue et al. 2005). The change in droplet size within a certain time period can be determined to high overall precision (±0.03 μm) by counting the number of overall intensity maxima observed in that period.

The temperature of the gas entering the levitation cell was measured with a thermocouple referenced to a platinum resistance thermometer (±0.02 °C; Omega), while the humidity was measured with a dew point hygrometer (±0.2 °C; General Eastern). The diffusion coefficient of water was taken from Pruppacher and Klett (1997, p. 503) and the thermal accommodation coefficient was set at 0.7 (Shaw and Lamb, 1999). The mass accommodation coefficient of H_2O was the primary free parameter in the least-squares fitting process. However, the dew point temperature was also varied in order to "fine tune" the quality of the fit. In all cases examined in this study, the value of T_{dew} determined via the least-squares fit was within ±0.2 °C of the measured dew point.

4. RESULTS AND DISCUSSION

Figure 3 shows a representative set of experimental results (points) along with the best-fit, simulated curves obtained from the droplet evaporation model. The green data point in each set represents the reference size. The measurements were performed at a pressure of 593 hPa and a cell temperature of -33.4 °C. Moisture was added to the carrier flow by passing a portion of the dry N_2 flow through a U-tube containing a packed bed of ice beads, resulting in a dew point temperature of -43.53 °C.

Table 1. Experimental conditions and measured mass accommodation coefficients for the droplets of Figure 3.

Drop	α	T_d(°C)	σ(μm)	T_{cell}(°C)	P (hPa)
3	0.225	-43.34	0.0152	-33.403	591
4	0.166	-43.56	0.01439	-33.3289	592
5	0.11	-43.52	0.01924	-33.2973	592
6	0.312	-43.59	0.01262	-33.5444	596
7	0.116	-44.63	0.05278	-33.2986	592

Table 1 summarizes the experimental conditions (T_{cell}, T_d, and P) for the droplets shown in Figure 3 and contains the experimentally determined α values and standard deviations (σ). The quality of the fit is evident from the standard deviation values, which are comparable to the overall precision of the optical sizing technique.
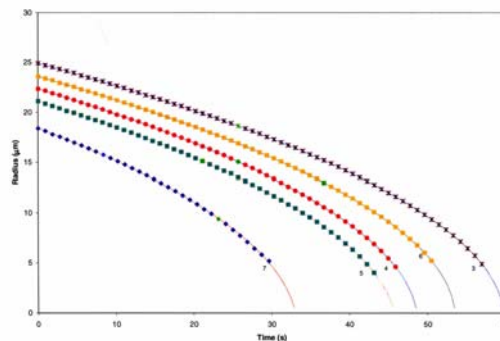

Figure 3. Experimental and simulated evaporation curves.

5. CONCLUSIONS

The results demonstrate that the simulated droplet evaporation curves fit the experimental data extremely well, thus validating the computer model. The model serves as a valuable diagnostic tool, which provides insight into the physical behavior of the droplets. Future work will focus on investigating the effect of experimental conditions on the measured value of α, with a view toward obtaining a better understanding of the surface kinetics of droplet growth and reconciling the discrepancies between various laboratory measurements.

REFERENCES

Lamb, D., A. M. Moyle, and W. H. Brune, 1996: The environmental control of individual aqueous particles in a cubic electrodynamic levitation system. *Aerosol Sci. Technol.*, **24**, 263-278.

Pruppacher, H. R., and J. D. Klett, 1997: Microphysics of Clouds and

Precipitation, 954 pp., Kluwer Academic Publishers.

Shaw, R. A. and D. Lamb, 1999: Experimental determination of the thermal accommodation and condensation coefficients of water. *J. Chem. Phys.*, **111**, 10659-10663.

Steiner, B., B. Berge, R. Gausmann, J. Rohmann, and E. Ruhl, 1999: Fast in situ sizing technique for single levitated liquid aerosols. *Applied Optics*, **38**, 1523-1529.

Xue, H., A. M. Moyle, N. Magee, J. Y. Harrington, and D. Lamb, 2005: Experimental Studies of Droplet Evaporation Kinetics: Validation of Models for Binary and Ternary Aqueous Solutions. *J. Atmos. Sci.*, **62**, 4310-4326.